determining our ability to culture these cell types in the future.

A finite proliferative capacity has been proposed to be an intrinsic property of normal cells, acting as a key regulatory mechanism for controlling inappropriate proliferation. Our results indicate that a reassessment of these ideas is required.

References and Notes

1. J. Campisi, *Eur. J. Cancer* **33**, 703 (1997).
2. A. G. Bodnar *et al.*, *Science* **279**, 349 (1998).
3. T. Kiyono *et al.*, *Nature* **396**, 84 (1998).
4. C. J. Sherr, R. A. DePinho, *Cell* **102**, 407 (2000).
5. J. P. Brockes, K. L. Fields, M. C. Raff, *Brain Res.* **165**, 105 (1979).
6. N. F. Mathon, D. S. Malcolm, M. C. Harrisingh, L. Cheng, A. C. Lloyd, data not shown.
7. G. P. Dimri *et al.*, *Proc. Natl. Acad. Sci. U.S.A.* **92**, 9363 (1995).
8. A. Di Leonardo, S. P. Linke, K. Clarkin, G. M. Wahl, *Genes Dev.* **8**, 2540 (1994).
9. B. B. McConnell, M. Starborg, S. Brookes, G. Peters, *Curr. Biol.* **8**, 351 (1998).
10. W. E. Wright, J. W. Shay, *Nature Med.* **6**, 849 (2000).
11. See *Science* Online (www.sciencemag.org/cgi/content/full/291/5505/872/DC1).
12. Passage 4, passage 10, and passage 20 Schwann cells (5×10^3 in each case) were seeded onto 90-mm PLL/laminin-coated dishes in Schwann cell medium supplemented with 20% conditioned medium collected from confluent Schwann cells. Schwann cells expressing dn-p53 were seeded as a positive control. Cells that successfully plated produced large colonies at very high efficiency (>50%). The plating and cloning efficiencies did not vary with passage number and were similar to those of cells expressing dn-p53.
13. F. Zindy, D. E. Quelle, M. F. Roussel, C. J. Sherr, *Oncogene* **15**, 203 (1997).
14. T. Kamijo *et al.*, *Cell* **91**, 649 (1997).
15. A. C. Lloyd *et al.*, *Genes Dev.* **11**, 663 (1997).
16. M. Serrano, A. W. Lin, M. E. McCurrach, D. Beach, S. W. Lowe, *Cell* **88**, 593 (1997).
17. A. C. Lloyd, *Curr. Opin. Genet. Dev.* **8**, 43 (1998).
18. L. Cheng, M. Khan, A. W. Mudge, *J. Cell Biol.* **129**, 789 (1995).
19. N. W. Kim *et al.*, *Science* **266**, 2011 (1994).

20. We thank M. Raff, A. Mudge, P. Mitchell, D. Tang, and I. Conlon for critical reading of the manuscript. A.C.L. is a Cancer Research Campaign (CRC) Senior Cancer Research Fellow. L.C. is funded by an MRC grant to A. Mudge.

20 October 2000; accepted 3 January 2001
Published online 19 January 2001;
10.1126/science.1056782
Include this information when citing this paper.

Control of Fusion Pore Dynamics During Exocytosis by Munc18

Richard J. Fisher,[1] Jonathan Pevsner,[2] Robert D. Burgoyne[1]*

Intracellular membrane fusion is mediated by the SNARE (soluble *N*-ethylmaleimide–sensitive factor attachment protein receptor) proteins. All vesicle transport steps also have an essential requirement for a member of the Sec1 protein family, including the neuronal Munc18-1 (also known as nSec1) in regulated exocytosis. Here, in adrenal chromaffin cells, we expressed a Munc18 mutant with reduced affinity for syntaxin, which specifically modified the kinetics of single-granule exocytotic release events, consistent with an acceleration of fusion pore expansion. Thus, Munc18 functions in a late stage in the fusion process, where its dissociation from syntaxin determines the kinetics of postfusion events.

Fusion of vesicles with target membranes is a key aspect of vesicular traffic and neurotransmitter release and is mediated by a core machinery of SNARE proteins (*1–3*). The three synaptic SNAREs (syntaxin 1, SNAP-25, and VAMP) are sufficient for bilayer fusion in vitro (*4*). This is, however, orders of magnitude slower than synaptic vesicle fusion, suggesting a role for additional factors (*5*). Members of the Sec1 family of proteins are required for all intracellular vesicular traffic steps (*6–10*), and the neuronal Munc18-1 protein (*11, 12*) is essential for synaptic vesicle exocytosis but not for constitutive exocytosis (*6, 8*). It binds to a closed conformation of syntaxin 1, which is unable to participate in the SNARE complex (*13–15*) and thus may control the addition of syntaxin into the complex. In current models, syntaxin assembles into a "loose" SNARE complex with Munc18 dissociation and the subsequent zippering of SNAREs into a "tight" complex immediately preceding membrane fusion (*2, 16*). Although SNARE complex assembly is crucial for membrane fusion, it is not known whether the complete assembly of the SNARE complex occurs before, during, or after fusion. Fusion proceeds via the formation of a reversible fusion pore (*17*), but the relation of the function of the SNARE proteins or Sec1 proteins to fusion pore opening and expansion is unknown.

We examined the effect of overexpression of wild-type Munc18 or a mutant form, $Arg^{39} \rightarrow Cys^{39}$ (R39C), on exocytosis using single-cell amperometry to resolve the frequency and kinetics of individual secretory granule release events. The R39C mutation was investigated for two reasons. First, the equivalent mutation in the *Drosophila* ortholog Rop, $Arg^{50} \rightarrow Cys^{50}$ in the F3 mutant (*9*), produces flies showing an increase in evoked neurotransmission (*8*). Second, the crystal structure of the Munc18–syntaxin 1 complex has revealed that Arg^{39} makes direct contact with Glu^{234} of syntaxin, leading to the prediction that the R39C mutation should weaken the binding interaction between the two proteins (*18*). A reduction of high-affinity binding of Munc18 containing the R39C mutation to syntaxin 1 was confirmed with an in vitro binding assay (*11, 19*) (Fig. 1A). When binding was assayed over a range of Munc18 protein concentrations (2 to 109 nM), the affinity of R39C for syntaxin was reduced by about fivefold in comparison to the wild type, from 6.5 to 35 nM, respectively. The R39C mutant (Fig. 1B) still bound the other Munc18 binding proteins Doc2 (*20*) and Mint1 (*21*) from a rat brain extract (*22*).

The effect of wild-type or R39C Munc18 on overall dense-core granule exocytosis was first assayed in PC12 cells by using transfection and coexpression of growth hormone (GH) (*23–25*). Transfection resulted in an ~10-fold overexpression of wild-type Munc18 (*26*). Overexpression of wild-type protein had no statistically significant effect on the extent of evoked exocytosis due to 10 μM free Ca^{2+} in permeabilized cells, but the R39C construct produced a significant (55%) inhibition (Fig. 1D). The difference in effect between the two proteins was not due to differences in expression, as both were expressed in virtually all transfected cells (Fig. 1C). We analyzed the effect of overexpression of the proteins in adrenal chromaffin cells using carbon-fiber amperometry to allow direct analysis of single-granule release events (*27–30*). Transfected chromaffin cells were detected by coexpression of green fluorescent protein (GFP), allowing untransfected cells in the same dishes to be used as controls. This ensured that all cells had been through the transfection protocol, and the same carbon fibers were used to record from transfected and control cells in each series of experiments. The cells were stimulated by local application of digitonin and Ca^{2+} to permeabilize the cells and allow Ca^{2+} to directly activate exocytosis (*24, 31*). Because the granules in these cells have a half-life of >15 days (*32*), this assay measured release

[1]Physiological Laboratory, University of Liverpool, Crown Street, Liverpool, L69 3BX, UK. [2]Department of Neurology, Kennedy Krieger Institute; and Department of Neuroscience, Johns Hopkins School of Medicine, 707 North Broadway, Baltimore, MD 21205, USA.

*To whom correspondence should be addressed. E-mail: Burgoyne@liverpool.ac.uk

from preformed granules. Overexpression of wild-type Munc18 or R39C had no effect on the overall evoked responses of the cells (Fig. 2) or on the average number of exocytotic events per cell. For wild-type protein, this was 7.43 ± 0.27 (n = 14 cells) for transfected cells versus 10.4 ± 3.1 (n = 10) for control cells, and for R39C, this was 6.32 ± 1.45 (n = 19) for transfected cells versus 6.88 ± 2.93 (n = 8) for control cells in the first 2 min after perfusion. In contrast, treatment with reserpine, an inhibitor of the vesicular monoamine transporter, to partially deplete granule catecholamine levels (*32*) had an obvious effect in reducing the peak amplitude of the spikes (Fig. 2, D and E).

Examination of the characteristics of the individual amperometric spikes, each reflecting catecholamine release from single granules (*27*), showed few effects of overexpression of wild-type Munc18 (*33*). In contrast, expression of R39C resulted in marked changes in spike characteristics, as compared to spikes from the corresponding control cells (Fig. 3). The mean height was unaffected, but the total charge, a reflection of the total catecholamine released per granule, was reduced by 45%, consistent with the inhibitory effect of the R39C protein on GH release from PC12 cells. This reduction in charge per spike is probably a consequence of a reduction in the half width of the spikes (Fig. 3C), i.e., the time over which release could occur. It is not due to a reduction in catecholamine content, as we also saw changes in the kinetics of release with decreases in both the rise and fall times of the spikes (Fig. 3, D and E). The reduction in charge per spike in R39C-expressing cells is not a consequence of the more rapid rate of release, as we found no correlation for individual spikes between the total charge and rise time under any conditions (*33*). A statistically significant correlation was found, however, between total charge and the half width of spikes (*33*), suggesting that the reduction in catecholamine release is a consequence of a shortening of the release time course. The change in the shape of spikes, showing the average parameters (Fig. 3F), was different in R39C-expressing cells as compared to the effect of depletion of vesicle catecholamine, where only the spike amplitude was changed (Fig. 3G).

The change in the rise and fall times seen above suggests an increase in the rate of opening of the initial fusion pore followed by its rapid closure in a kiss-and-run–type fusion event (*34*). This effect was specific, as amperometric spikes were not modified by reduction in SNARE availability by clostridial neurotoxin treatment (*24*) or by expression of a dominant-negative α-SNAP mutant that can interact irreversibly with multiple SNARE proteins (*35*). The kinetics of single release events can be modified, however, under specific conditions (*24, 30*), including treatment with phorbol esters that increases fusion pore opening rates in other cell types (*36*). The effect of expression of R39C is identical to the effect of activation of protein kinase C (PKC) (*24*). PKC phosphorylation of Munc18 reduces its binding to syntaxin 1 (*37*), so that the phosphorylated form behaves like R39C, suggesting that phosphorylation of Munc18 could regulate kiss-and-run fusion in regulated exocytosis.

The reduction in release from dense-core granules following R39C expression can be reconciled with the findings in *Drosophila*, where the mutation leads to increased neurotransmission (*8*). The consequence of the mutation could be to increase the rate of neurotransmitter release and the rate of rise in neurotransmitter concentration in the synaptic cleft. This could explain the increase in postsynaptic current and the reduction in neurotransmission failures in the *Drosophila* F3 mutant. The reduced affinity of R39C for syntaxin suggests that R39C would be able to dissociate more easily from syntaxin than would wild-type protein and R39C would allow more efficient assembly of the "tight" SNARE complex (*18*). If this is the case, then our data suggest that dissociation of Munc18 and the full SNARE complex assembly occur very late, either during membrane fusion or during fusion pore expansion. Alternatively, dissociation of Munc18 may be important to allow it to directly exert an effect on the fusion process independent of syntaxin 1 either alone or via a downstream effector. The yeast Sec1 has been suggested to have a late role in constitutive exocytosis after SNARE complex assembly (*38, 39*), consistent with this interpretation. Accumulating evidence suggests that fusion pore dynamics can be regulated (*40–44*). Our data show that Munc18 plays a late role in membrane fusion and has a key function in fusion pore dynamics, and the data suggest that it may be a target for the control of kiss-and-run fusion in exocytosis.

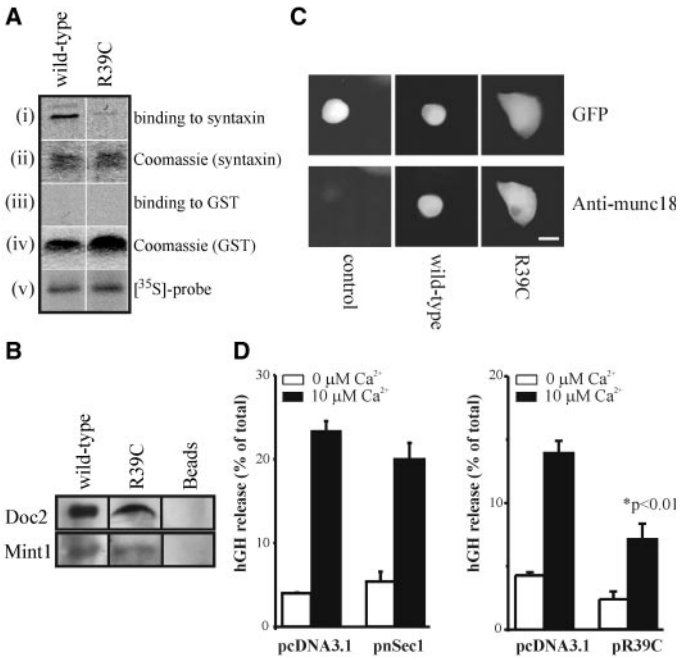

Fig. 1. Reduced binding of Munc18 R39C to syntaxin and the effect of expression on evoked GH release. (**A**) Wild-type Munc18 and the R39C mutant were labeled by in vitro transcription and translation in the presence of [^{35}S]methionine, and binding to GST–syntaxin 1A or GST control was assayed. (i), (iii), and (v) show autoradiograms and (ii) and (iv) show Coomassie blue–stained proteins. No binding of Munc18 was seen in GST control incubations. From a quantitative analysis, the binding of R39C to GST–syntaxin 1A was reduced to 1% of the wild-type binding in three experiments. (**B**) Pull-down assay showing the binding of Doc2 and Mint1 from rat brain membrane extracts to GST-Munc18 (wild type), GST-Munc18 (R39C), and control beads. (**C**) Demonstration of overexpression of wild-type or R39C Munc18 in adrenal chromaffin cells that were cotransfected with GFP and stained with anti-Munc18 [anti-rbSec1A (*45*)] at a concentration (1:200) that gave only background staining of control cells (left) transfected with a vector. The scale bar represents 10 μm. (**D**) PC12 cells were cotransfected with a control vector or plasmids encoding wild-type Munc18 or the R39C mutant along with a plasmid encoding human GH. Three days after transfection, the cells were permeabilized with digitonin and challenged with or without Ca^{2+} for 10 min. Released human GH was assayed and expressed as a percentage of total cell content (n = 6). Error bars indicate SEM.

References and Notes

1. R. B. Sutton, D. Fasshauer, R. Jahn, A. T. Brunger, *Nature* **395**, 347 (1998).
2. Y. A. Chen, S. J. Scales, S. M. Patel, Y.-C. Doung, R. H. Scheller, *Cell* **97**, 165 (1999).
3. T. Sollner *et al.*, *Nature* **362**, 318 (1993).
4. T. Weber *et al.*, *Cell* **92**, 759 (1998).
5. R. Jahn, T. C. Sudhof, *Annu. Rev. Biochem.* **68**, 863 (1999).
6. M. Verhage *et al.*, *Science* **287**, 864 (2000).
7. P. Novick, R. Schekman, *Proc. Natl. Acad. Sci. U.S.A.* **76**, 1858 (1979).
8. M. N. Wu, J. T. Littleton, M. A. Bhat, A. Prokop, H. J. Bellen, *EMBO J.* **17**, 127 (1998).
9. S. D. Harrison, K. Broadie, J. van de Goor, G. M. Rubin, *Neuron* **13**, 555 (1994).
10. M. R. Peterson, C. G. Burd, S. D. Emr, *Curr. Biol.* **9**, 159 (1999).

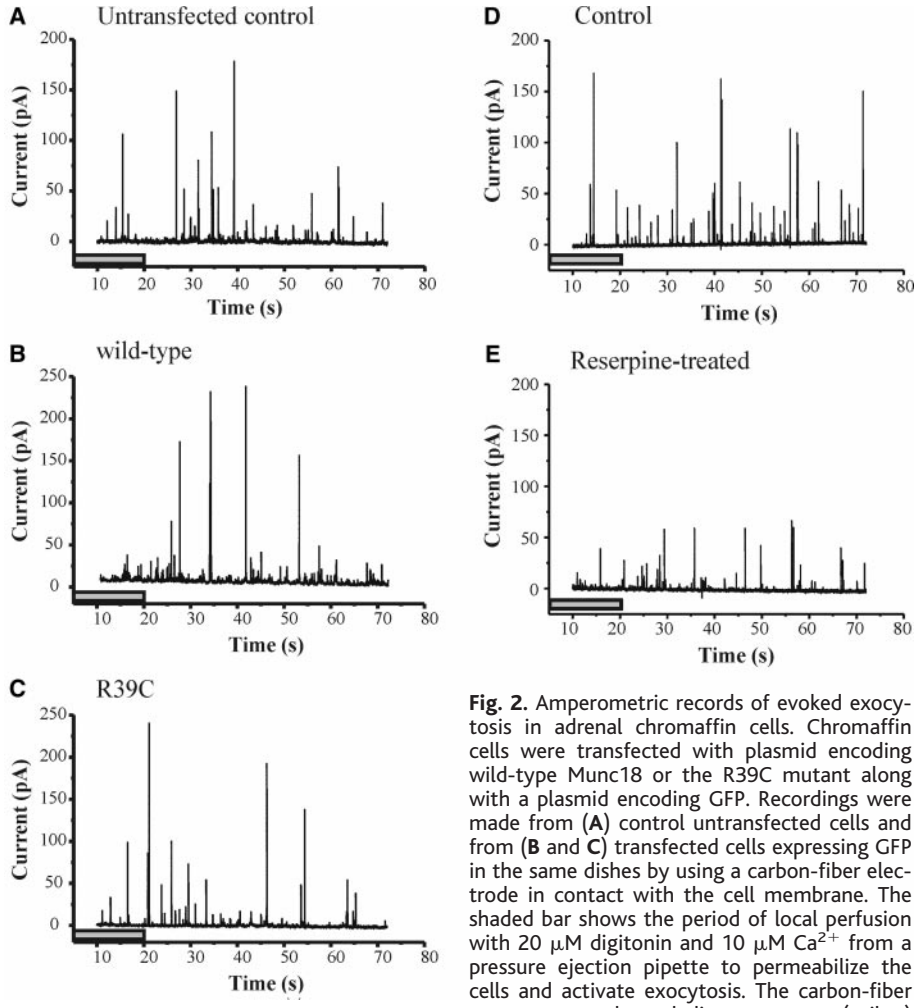

Fig. 2. Amperometric records of evoked exocytosis in adrenal chromaffin cells. Chromaffin cells were transfected with plasmid encoding wild-type Munc18 or the R39C mutant along with a plasmid encoding GFP. Recordings were made from (**A**) control untransfected cells and from (**B** and **C**) transfected cells expressing GFP in the same dishes by using a carbon-fiber electrode in contact with the cell membrane. The shaded bar shows the period of local perfusion with 20 μM digitonin and 10 μM Ca^{2+} from a pressure ejection pipette to permeabilize the cells and activate exocytosis. The carbon-fiber amperometry showed discrete events (spikes) due to catecholamine release from individual secretory granules, and the responses appeared to be similar for each condition. Overexpression of wild-type Munc18 or R39C did not affect spike amplitude. In contrast, reserpine treatment to deplete vesicle catecholamine reduced spike amplitude in comparison with controls (**D** and **E**). The latter data are typical of 11 control and 14 reserpine-treated cells.

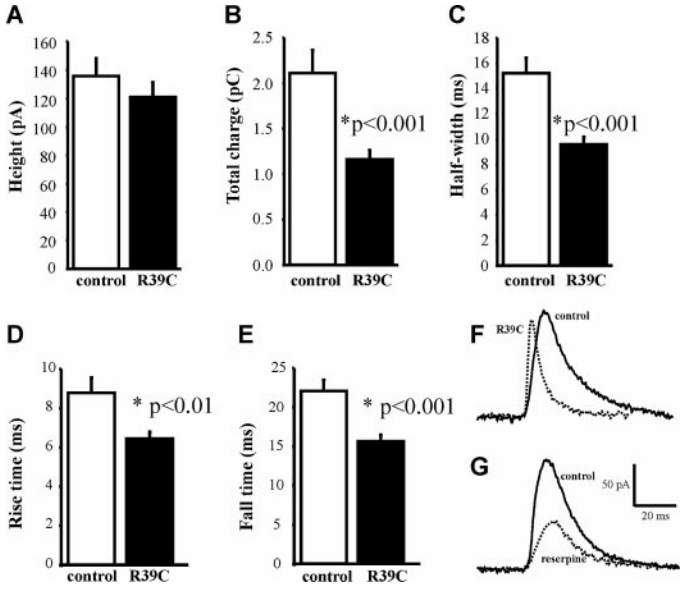

Fig. 3. Analysis of single amperometric spikes from cells expressing Munc18 R39C. No change in spike height was seen in R39C transfected cells as compared to (**A**) the respective controls, but statistically significant reductions were observed in (**B**) total charge, (**C**) half width, (**D**) rise time, and (**E**) fall time of the spikes. The data are derived from experiments on 8 (53 spikes) control and 19 (117 spikes) transfected cells. Error bars indicate SEM. (**F**) Spikes with average parameters from control and R39C-expressing cells. (**G**) Spikes from control and reserpine-treated (0.5 μM, for 16 hours) cells.

11. J. Pevsner, S. C. Hsu, R. Scheller, *Proc. Natl. Acad. Sci. U.S.A.* **91**, 1445 (1994).
12. Y. Hata, C. A. Slaughter, T. C. Sudhof, *Nature* **366**, 347 (1993).
13. J. Pevsner *et al.*, *Neuron* **13**, 353 (1994).
14. B. Yang, M. Steegmaier, L. C. Gonzalez, R. H. Scheller, *J. Cell Biol.* **148**, 247 (2000).
15. I. Dulubova *et al.*, *EMBO J.* **18**, 4372 (1999).
16. T. Xu *et al.*, *Cell* **99**, 713 (1999).
17. M. Lindau, W. Almers, *Curr. Opin. Cell Biol.* **7**, 509 (1995).
18. K. M. S. Misura, R. H. Scheller, W. I. Weis, *Nature* **404**, 355 (2000).
19. For assay of syntaxin binding, wild-type Munc18 or the R39C mutant was radiolabeled by in vitro transcription and translation in the presence of [^{35}S]methionine and incubated with glutathione *S*-transferase (GST)–syntaxin 1A that was immobilized on glutathione-Sepharose beads, as described previously (*13*). Bound proteins were eluted in SDS sample buffer, electrophoresed, and analyzed by autoradiography or Coomassie blue staining. For determination of binding affinity, bound unlabeled Munc18 was detected by Western blotting. For assay of binding of Doc2 and Mint1, GST-Munc18 was immobilized on glutathione-Sepharose beads and incubated with an extract of rat brain membranes. Bound proteins were detected by Western blotting. All primary antibodies were obtained from Transduction Laboratories (Lexington, KY).
20. M. Verhage *et al.*, *Neuron* **18**, 453 (1997).
21. M. Okamoto, T. C. Sudhof, *J. Biol. Chem.* **272**, 31459 (1997).
22. L. P. Haynes, A. Morgan, R. D. Burgoyne, *Biochem. J.* **342**, 707 (1999).
23. P. F. Wick, R. A. Senter, L. A. Parsels, M. D. Uhler, R. W. Holz, *J. Biol. Chem.* **268**, 10983 (1993).
24. M. E. Graham, R. J. Fisher, R. D. Burgoyne, *Biochimie* **82**, 469 (2000).
25. A plasmid containing the coding sequence for rat Munc18-1 in pcDNA3 (pnSec1) was described previously (*26*) and was used as the template in site-directed mutagenesis to produce the R39C construct (pR39C). The assay of release from transfected PC12 cells used a modification of the GH release assay following transient transfection (*23*). PC12 cells were maintained in culture in 24-well trays and were transiently cotransfected, as previously described (*24*), with Lipofectamine (Gibco-BRL). After the removal of culture medium, cells were washed with Krebs-Ringer buffer and permeabilized for 6 min with 20 μM digitonin before challenge with or without 10 μM Ca^{2+} for 10 min. Buffer samples and cells were assayed for GH levels by using an enzyme-linked immunosorbent assay kit (Boehringer Mannheim) according to the manufacturer's instructions.
26. M. E. Graham, A. W. Sudlow, R. D. Burgoyne, *J. Neurochem.* **69**, 2369 (1997).
27. T. J. Schroeder *et al.*, *Biophys. J.* **70**, 1061 (1996).
28. R. M. Wightman, T. J. Schroeder, J. M. Finnegan, E. L. Ciolkowski, K. Pihel, *Biophys. J.* **68**, 383 (1995).
29. Freshly isolated bovine adrenal chromaffin cells were plated on non–tissue-culture-treated 10-cm Petri dishes at a density of 1×10^6 per milliliter and left overnight. The following day, nonattached cells were harvested by centrifugation and resuspended in growth medium at a density of 1×10^7 per milliliter. Twenty micrograms of pEGFP (plasmid encoding enhanced GFP) (Clontech, Basingstoke, Hampshire, UK) and 20 μg of either pnSec1 or pR39C were added per milliliter of cells, and the mixture was electroporated at 250 V and 975 μF for one pulse, using a Bio-Rad Gene Pulser II (Bio-Rad). Cells were rapidly diluted and grown on 35-mm Petri dishes in a final volume of 3 ml of growth medium for an additional 3 to 5 days.
30. For carbon-fiber amperometry, the cells were washed three times with Krebs-Ringer buffer [145 mM NaCl, 5 mM KCl, 1.3 mM $MgCl_2$, 1.2 mM NaH_2PO_4, 10 mM glucose, and 20 mM Hepes (pH 7.4)] and incubated in bath buffer [139 mM potassium glutamate, 20 mM Pipes, 0.2 mM EGTA, 2 mM adenosine 5′-triphosphate (ATP), and 2 mM $MgCl_2$ (pH 6.5)]. Transfected cells were identified as those expressing EGFP. For reserpine treatment, 0.5 μM reserpine was added to the medium, and recording began after 16 hours. A 5-μm-diameter carbon-fiber electrode was moved into contact with the

cell surface. A glass micropipette filled with cell permeabilization/stimulation buffer [139 mM potassium glutamate, 20 mM Pipes, 5 mM EGTA, 2 mM ATP, 2 mM $MgCl_2$, 20 mM digitonin, and 10 μM free Ca^{2+} (pH 6.5)] was positioned on the opposite side from the carbon fiber, ~60 μm from the cell. For stimulation of the cells, the buffer was pressure-ejected onto the cell for 20 s. Amperometric responses were monitored with a VA-10 amplifier (NPI Electronic, Tamm, Germany), collected at 4 kHz, digitized with a Digidata 1200B acquisition system, and monitored online with the AxoScope 7.0 program (Axon Instruments, Foster City, CA). Data were subsequently analyzed with an automated peak detection and analysis protocol within the program Origin (Microcal, Northampton, MA). Spikes were selected for analysis if they had a base width greater than 6 ms and an amplitude greater than 40 pA, so that the analyses were confined to spikes arising immediately beneath the carbon fiber.

31. M. E. Graham, R. D. Burgoyne, *J. Neurosci.* **20**, 1281 (2000).
32. J. J. Corcoran, S. P. Wilson, N. Kirshner, *J. Biol. Chem.* **259**, 6208 (1984).
33. Supplementary data are available at www.sciencemag.org/cgi/content/full/291/5505/875/DC1.
34. R. Fesce, F. Grohovaz, F. Valtorta, J. Meldolesi, *Trends Cell Biol.* **4**, 1 (1994).
35. R. J. O. Barnard, A. Morgan, R. D. Burgoyne, *J. Cell Biol.* **139**, 875 (1997).
36. S. Scepek, J. R. Coorssen, M. Lindau, *EMBO J.* **17**, 4340 (1998).
37. Y. Fujita *et al.*, *J. Biol. Chem.* **271**, 7265 (1996).
38. C. M. Carr, E. Grote, M. Munson, F. M. Hughson, P. J. Novick, *J. Cell Biol.* **146**, 333 (1999).
39. E. Grote, C. M. Carr, P. J. Novick, *J. Cell Biol.* **151**, 439 (2000).
40. G. Alvarez de Toledo, R. Fernandez-Chacon, J. M. Fernandez, *Nature* **363**, 554 (1993).
41. E. Ales *et al.*, *Nature Cell Biol.* **1**, 40 (1999).
42. R. Fernandez-Chacon, G. Alvarez de Toledo, *FEBS Lett.* **363**, 221 (1995).
43. J. Hartmann, M. Lindau, *FEBS Lett.* **363**, 217 (1995).
44. M. A. Cousin, P. J. Robinson, *J. Neurochem.* **75**, 1645 (2000).
45. E. P. Garcia, P. S. McPherson, T. J. Chilcote, K. Takei, P. De Camilli, *J. Cell Biol.* **129**, 105 (1995).

46. We thank P. De Camilli (Yale University) for the gift of anti-rbSec1A and L. Frelin (John Hopkins Medical School) for technical assistance with syntaxin binding assays. This work was supported by the Wellcome Trust, R.J.F. was supported by a Wellcome Trust Prize Studentship, and J.P. was supported by NIH grant RO1 NS36670-01A1.

17 November 2000; accepted 8 January 2001

Bakers' Yeast, a Model for Fungal Biofilm Formation

Todd B. Reynolds and Gerald R. Fink*

Biofilms are formed by the aggregation of microorganisms into multicellular structures that adhere to surfaces. Here we show that bakers' yeast *Saccharomyces cerevisiae* can initiate biofilm formation. When grown in low-glucose medium, the yeast cells adhered avidly to a number of plastic surfaces. On semi-solid (0.3% agar) medium they formed "mats": complex multicellular structures composed of yeast-form cells. Both attachment to plastic and mat formation require Flo11p, a member of a large family of fungal cell surface glycoproteins involved in adherence. The ability to study biofilm formation in a tractable genetic system may facilitate the identification of new targets for antifungal therapy.

Many microorganisms have the ability to grow in association with a surface in an aggregate of cells called a biofilm. Biofilms have taken center stage with the increasing recognition of their role in human infections. Pathogenic bacteria and fungi can form biofilms on the inert surfaces of implanted prosthetic devices such as catheters and on fragments of dead tissue. In the protected microenvironment of a biofilm, the pathogens are more resistant to antimicrobial therapies (*1*, *2*).

Little is known about fungal biofilms because many of the organisms that form these structures are not amenable to genetic approaches (*1*, *3*). In search of a model system for fungal biofilms, we investigated whether the well-characterized bakers' yeast *S. cerevisiae* can form biofilms. Bacteria are said to form biofilms if they adhere to plastic (*1*). We found that *S. cerevisiae* adhered to polystyrene plates (Fig. 1), and the cells remained adherent even after repeated washes (*4*). The yeast cells also adhered to polypropylene and, to a lesser degree, to polyvinylchloride (PVC) (*5*). These results suggested that *S. cerevisiae* can initiate biofilm formation.

The adherence of yeast to plastic was enhanced as the glucose concentration was lowered, but it was reduced in the complete absence of glucose, suggesting that there is a requirement for active metabolism (Fig. 1A). Diploid cells did not adhere as well as haploids in this assay (Fig. 1, B and C). Examination of the attached cells by microscopy revealed that they were round yeast-form cells (Fig. 1D).

Because bacterial biofilm formation requires cell surface adhesins (*1*), we disrupted *FLO11*, a yeast gene encoding a cell surface glycoprotein that is required for adhesion to agar (*6*, *7*), and *FLO8*, a yeast gene that encodes a regulatory protein required for *FLO11* expression (*8*). Isogenic strains (*9*) lacking either *FLO11* (*flo11*Δ; Fig. 1, B to D) or *FLO8* (*flo8*Δ) adhered poorly to polystyrene even in low glucose.

The role of Flo11p in the adherence of *Saccharomyces* to plastic may be similar to that of the glycopeptidolipids (GPLs) expressed on the cell surface of *Mycobacterium smegmatis*, a nonflagellated bacterium. *Mycobacterium smegmatis* mutants defective in GPL synthesis are defective in both biofilm formation and in a distinct colonial behavior called "sliding motility," suggesting an intimate connection between the two phenotypes (*10*, *11*). Sliding motility is defined as a form of surface motility " . . . produced by the expansive forces of the growing bacterial population in combination with cell surface properties that favor reduced friction between the cells and the substrate" (*10*, p. 4348).

To determine whether *Saccharomyces* displays a *FLO11*-dependent phenotype similar to sliding motility, we inoculated strains onto YPD plates containing 0.3% rather than 2% agar. On this low agar concentration, *S. cerevisiae* exhibited an elaborate pattern of multicellular growth resulting in a confluent mat (Fig. 2). The low concentration of agar required for formation of this structure is similar to that which triggers the sliding motility of *M. smegmatis* (*10*, *11*).

When inoculated in the center of 0.3% agar plates, *S. cerevisiae* produced a flat mat covering a larger surface than that of the same strain inoculated on 2% agar (Fig. 2, G and H). This structure grew in a radial form both on circular and square petri dishes and ultimately covered most of the agar, achieving a mean diameter of 7.8 ± 0.57 cm after 13 days (*12*). The mature structure had a central hub made of a network of cables (Fig. 3A) and radial spokes emanating from the hub. Spokes formed reproducibly within a defined range with a mean of 14.4 spokes ± 4.5 (*12*). The spokes and hub were more distinct at 25°C than at 30°C. The number of cells produced by mat formation on 0.3% agar was 7.6 times greater (day 12) than that in a colony produced on 2% agar by the same strain (*13*). The formation of mats and spokes, like adherence to plastic, was sensitive to glucose concentration; reduction in the glucose concentration resulted in a more rapid formation of spokes and hubs (*14*).

The ability of *S. cerevisiae* to form the mat structure was *FLO11*-dependent. Growth of a *flo11*Δ strain on a 0.3% agar plate produced a mass of cells with a smaller diameter and without the characteristic morphology of a *FLO11* mat (Figs. 2L and 3B). The *FLO11* mat after 12 days on 0.3% agar contained ~1.6 times the number of cells as a *flo11*Δ strain, whereas on

Whitehead Institute for Biomedical Research and Massachusetts Institute of Technology, Nine Cambridge Center, Cambridge, MA 02142, USA.

*To whom correspondence should be addressed. E-mail: gfink@wi.mit.edu